Exploring the thermoelectric response of novel polymorphs of ZnO for renewable energy applications using first-principles approaches

SAIRA SHABBIR[a], A. SHAARI[a], BAKHTIAR UL HAQ[b,*], S. ALFAIFY[b], R. AHMED[a,c], M. AHMED[c]
[a]*Department of Physics, Faculty of Science, Universiti Teknologi Malaysia, UTM Skudai, 81310 Johor, Malaysia*
[b]*Advanced Functional Materials & Optoelectronics Laboratory (AFMOL), Department of Physics, Faculty of Science, King Khalid University, P.O. Box 9004, Abha, Saudi Arabia*
[c]*Center for High Energy Physics, University of the Punjab, Quid-e-Azam Campus Lahore-54590 Pakistan*

The inexpensive, earth abundant, and non-toxic thermoelectric materials are relentlessly demanded to realize the dream of sustainable energy and overcome the energy crisis. To do so, a lot of studies are being conducted on different materials at different levels. However, the energy crisis is still a big challenge. Some polymorphs of zinc oxide (ZnO) being cheaper, non-toxic, and exhibiting good thermoelectric response at high temperatures have shown its adequate potential to play a role in sustainable energy technologies. In this study, we attempt to explore the thermoelectric response of different types of ZnO polymorphs named as *sphalerite*, *wurtzite*, *CsCl*, *NiAs*, *GeP*, *BeO*, *5-5* type versus chemical potential and temperature and the study is carried out by full-potential (FP) linearised (L) augmented plane wave (APW) plus local orbitals (*lo*) (FP-L(APW+*lo*) approach structured within density functional theory (DFT) and Boltzmann transport theory. Our obtained results of thermoelectric power factors for *sphalerite*, *wurtzite*, *CsCl*, *NiAs*, *GeP*, *BeO*, *5-5* type of the polymorphs of ZnO are recorded as 8.04×10^{11} W/mK^{2}s, 7.01×10^{11} W/mK^{2}s, 11.7×10^{11} W/mK^{2}s, 4.90×10^{11} W/mK^{2}s, 4.97×10^{11} W/mK^{2}s, 2.28×10^{11} W/mK^{2}s, and 5.31×10^{11} W/mK^{2}s respectively. Hence, the considered polymorphs of ZnO have been found to exhibiting the great potential to replace expensive, rare, and toxic thermoelectric materials.

(Received October 2, 2020; accepted June 11, 2021)

Keywords: ZnO Polymorphs, Thermoelectric properties, Density functional theory, Seebeck coefficient, Power factor

1. Introduction

Undoubtedly, the demand for clean, sustainable, and renewable energy resources is one of the most concerning issues in the whole world. Thermoelectric (TE) materials having the capability to change the waste heat energy to electrical power are believed to have the potential to meet the energy challenges. Additionally, TE devices play a significant role in minimizing the effect of harmful gases emitted by conventional energy resources as well [1-5]. The efficiency of material for thermoelectric applications is characterized by its figure of merit (*ZT*). It is a dimensionless quantity and is defined as

$$ZT = \frac{S^2 \sigma T}{\kappa} \quad (1)$$

where "*S*", "σ", "*T*" and "κ" are Seebeck coefficient, electrical conductivity, absolute temperature, and thermal conductivity respectively. It is clear from Equation (1) that the electrical conductivity (σ) and Seebeck coefficient (*S*) are directly proportional to *ZT*, and thermal conductivity (κ) is inversely proportional to *ZT*, therefore, for a large figure of merit, higher values of Seebeck coefficient and electrical conductivity and a small value of thermal conductivity is required [6, 7]. However, materials exhibiting such a favourable combination are hard to find. Therefore, among the common approaches adopted to achieve large *ZT* values, is exploring new polymorphs of the existing material.

Zinc oxide (ZnO) material, a member of the II-VI semiconductor family, is extensively studied due to its unique physical properties suitable for technological applications. In recent years, ZnO has received growing attention of researchers for advanced thermoelectric applications due to its low-cost production, high Seebeck coefficient, non-toxic behavior, and abundant availability in nature. Although its stable *wurtzite* and meta-stable zincblende and rocksalt phases at ambient conditions are studied intensively [8-27], recently, various modified polymorphs of ZnO such as *sphalerite*, *CsCl*, *NiAs*, *GeP*, *BeO*, *5-5* types have been analyzed at different pressures and realized as great potential candidates for the next generation semiconductors [27-31]. This includes our study where we comprehensively examined the potential of the novel polymorphs of ZnO for optoelectronic applications [31]. These polymorphs have been reported as stable as *wurtzite* structure, however, there is a lack of availability of literature to realize the potential of these new polymorphs towards thermoelectric response and for clean energy applications. To gain insight view about thermoelectric behavior of new modified polymorphs of

ZnO as well as to make comparison with the stable and already established structure, *wurtzite* of ZnO, we investigate the thermoelectric properties of seven polymorphs that is *sphalerite*, *wurtzite*, *CsCl*, *NiAs*, *GeP*, *BeO*, *5-5* type using DFT and Boltzmann transport theory-based computational approaches.

In this study, the electronic energy bandgap structures of *sphalerite*, *wurtzite*, *CsCl*, *NiAs*, *GeP*, *BeO*, *5-5* type polymorphs of ZnO are determined by employing the WIEN2k crystalline computational code based on FP-L(APW+*l*o) method [32] which is developed within DFT. For exchange-correlation functional, in conjunction with Perdew-Burke Ernzerhof generalized gradient approximation (PBE-GGA), Trans-Blaha (TB) modified Becke-Johnson (mBJ) approach is also used to determine the electronic band structures. The thermoelectric properties of the considered polymorphs of the ZnO are calculated by employing the semi-classical Boltzmann transport theory while considering the relaxation time (τ) as a constant as implemented in the BoltzTraP code [33]. In thermoelectric properties, we have determined the electrical conductivities, thermal conductivities, Seebeck coefficients, power factors and figure of merit of *sphalerite*, *wurtzite*, *CsCl*, *NiAs*, *GeP*, *BeO*, *5-5* type of the ZnO polymorphs at room temperature (300 K) vs. chemical potential and also the same thermoelectric parameters have been calculated at different temperatures (0 to 1000 K).

2. Computational detail

The band structure calculations required to assess thermoelectric characteristics of *sphalerite*, *wurtzite*, *CsCl*, *NiAs*, *GeP*, *BeO*, *5-5* type polymorphs of the ZnO are conducted via FP-L(APW+lo) method framed within DFT and realized in WIEN2k computational package [32]. In this approach of computation, simulated unit-cell is treated by dividing it into the interstitial region and non-overlapping spheres. In the interstitial region, plane waves are used as a basis set whereas, in the atomic spheres (Muffin tin spheres, MT) region, atomic like wave function is used. The input data, to simulate the unit-cell for performing computations to obtain optimized lattice parameters, was taken from the literature [29]. The l_{max}= 10 was used to expand the wave function in the spherical region, whereas in the intestinal region $K_{max}=8.0/R_{MT}$ $(Ryd)^{1/2}$ was considered to get suitable convergence of the energy eigenvalues, and radii of atomic spheres (R_{MT}) for Zn atom 1.93 a.u, 1.80 a.u., 2.15 a.u., 1.95 a.u., 1.87 a.u., 1.78 a.u., 1.83 a.u., and for O 1.63 a.u., 1.55 a.u., 1.85 a.u., 1.68 a.u., 1.61 a.u., 1.53 a.u., 1.57 a.u. were used for the *sphalerite*, *wurtzite*, *CsCl*, *NiAs*, *GeP*, *BeO*, *5-5* type of the polymorphs of ZnO respectively. Similarly, $G_{max}=16$ $a.u^{-1}$ value was used for the Fourier expanded charge density for all polymorphs of the ZnO investigated in this study. For the band structure calculations, 1000 k-points were used to perform integration over the whole irreducible Brillouin zone. To separate the core states from the valence states, cutoff energy value equal to -6.0 Ryd was set. By using the above-said parameters, convergence criteria of 10^{-5} Ryd were attained for energy eigenvalues per unit cell in our self-consistent calculations. As TB-mBJ potential is reported to be more appropriate for insulators as well as semiconductors, therefore in addition to PBE-GGA, a combination of PBE-GGA & TB-mBJ exchange-correlation potential is also employed to calculate more accurate results of electronic bandgap values to achieve reliable results for thermoelectric properties as well [3, 25-27, 31, 34-51].

We have used the electronic band structure results which were obtained by using the above-described computational details to calculate the thermoelectric properties like thermal conductivity per relaxation time (κ/τ), electrical conductivity per relaxation time (σ/τ), Seebeck coefficients (S), and power factor (P.F) for *sphalerite*, *wurtzite*, *CsCl*, *NiAs*, *GeP*, *BeO*, *5-5* type of the polymorphs of ZnO. These thermoelectric properties have been determined by employing semi-classical Boltzmann transport theory implemented in the BoltzTraP code [33]. Equations (2) and (3) can be used to determine the thermoelectric coefficients, for instance, electrical conductivity ($\sigma_{\alpha\beta}$) and Seebeck coefficient ($S_{\alpha\beta}$) as a function of temperature (T) and chemical potential (μ),

$$\sigma_{\alpha,\beta}(T,\mu) = \frac{1}{\Omega}\int \sum_{\alpha,\beta}(\varepsilon)\left[\frac{-\partial f_0(T,\varepsilon,\mu)}{\partial \varepsilon}\right] d\varepsilon \qquad (2)$$

$$S_{\alpha,\beta}(T,\mu) = \frac{1}{eT\Omega\sigma_{\alpha,\beta}(T,\mu)}\int (\varepsilon-\mu)\sum_{\alpha,\beta}(\varepsilon)\left[\frac{-\partial f_0(T,\varepsilon,\mu)}{\partial \varepsilon}\right] d\varepsilon \qquad (3)$$

where the symbols α and β represent to the cartesian indexing and "f_0", "Ω" and "e" are used Fermi Dirac distribution function for the charge carriers, unit cell volume, and electronic charge respectively. In Equation (2) and (3), the term $\sum_{\alpha,\beta}(\varepsilon)$ is used for the transport distribution function for projected energy and can be said to be a key term of the Equation (2) and (3). $\sum_{\alpha,\beta}(\varepsilon)$ can be written as followed:

$$\sum_{\alpha,\beta}(\varepsilon) = \frac{e2}{N}\sum_{i,k}\tau v_\alpha(i,k)v_\beta(i,k)\delta\left(\varepsilon-\varepsilon_{i,k}\right) \qquad (4)$$

where "N", "i", "k", "τ" and $v_\alpha(i,k) = \frac{1}{\hbar}\frac{\partial \varepsilon_{i,k}}{\partial k_\alpha}$ in equation (4) has been used for the total numbers of k-points taken to perform integration over the Brillouin Zone (BZ), band index, wave vector, relaxation time, and group velocity respectively. In this approach of calculations, the thermoelectric parameters such as power factor ($S^2\sigma/\tau$), thermal conductivity(κ/τ) and electrical conductivity (σ/τ) are determined with respect to relaxation time [7, 52].

3. Results and discussion

The crystal structures and the band structure diagrams for *sphalerite*, *wurtzite*, *CsCl*, *NiAs*, *GeP*, *BeO*, *5-5* type of

the ZnO polymorphs along with energy bandgap values are available in the supplementary material. It can be seen from figure. S2 that *sphalerite*, *wurtzite*, *NiAs*, *BeO*, and *5-5* type structures have direct bandgap with band gap energies 2.670 eV, 2.901 eV, 2.986 eV, 3.04 eV, 3.127 eV whereas *GeP* and *CsCl* type exhibit indirect bandgap with a bandgap of 2.648 eV and 1.853 eV. In thermoelectric properties, we have calculated the thermal conductivity (κ), electrical conductivity (σ/τ), Seebeck coefficients (S), and power factor (P.F) against chemical potential and temperature. First, we will discuss the thermoelectric properties vs. the chemical potential at room temperature (300 K) and then vs. temperature in the range of 0-1000 K.

The electrical conductivity of a material is straightforwardly related to size and the nature of the electronic bandgap energy of the material. The electrical conductivities (σ/τ), and the onset of σ/τ against chemical potential ($\mu(eV)$) for *sphalerite*, *wurtzite*, *CsCl*, *NiAs*, *GeP*, *BeO*, *5-5* types of the polymorphs of ZnO at room temperature (300K) have been presented in Fig. 1 (a) respectively. The chemical potential has been set at 0 eV as denoted by the dotted line in Fig. 1. The positive values of $\mu(eV)$ represent the *n*-type (electron excess region) while -ve values reflect the *p*-type region (the region with an excess of the hole).

In Fig. 1 (a), the onset of σ/τ for *n*-type doping occurs at 3.2 eV for *wurtzite*, 2.8 eV for *sphalerite*, 2.6 eV for *GeP* type, 3.5 eV for *5-5* type, 3.4 eV for *NiAs*, 3.3 eV for *BeO* type and 1.81 eV for *CsCl* type of ZnO polymorphs and the results are found in good agreement with their electronic band gap values presented in Table S1 of supplementary material. The σ/τ of *wurtzite*, *sphalerite*, *NiAs*, *GeP*, and *BeO* types of ZnO polymorphs have been found larger for *n*-type doping whereas *CsCl*- and 5-5- types polymorph of ZnO exhibited higher σ/τ for *p*-type doping. This indicates the *n*-type nature of *wurtzite*, *sphalerite*, *NiAs*, *GeP*, and *BeO* types of ZnO polymorphs and *p*-type nature of *CsCl*- and 5-5- types of ZnO. The *n*-type nature of ZnO in the wurtzite phase has also been reported in the literature [53, 54]. The obtained results for the maximum values of σ/τ and the corresponding chemical potential values for *sphalerite wurtzite*, *CsCl*, *NiAs*, *GeP*, *BeO*, and *5-5* type polymorphs of ZnO are tabulated in Table 1. In all the above-mentioned polymorphs of the ZnO, the *GeP* type of ZnO showed larger electrical conductivity due to the smaller bandgap.

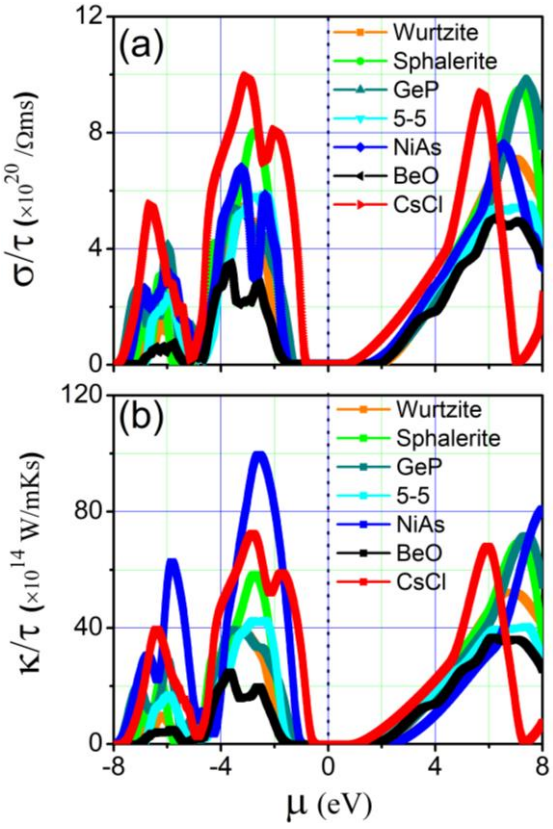

Fig. 1. σ/τ (a) and κ/τ (b) for wurtzite type, sphalerite type, GeP type, 5-5 type, NiAs type, BeO type and CsCl type ZnO polymorphs against chemical potential (μ) (color online)

The thermal conductivities (κ/τ) against chemical potential ($\mu(eV)$) for *sphalerite wurtzite*, *CsCl*, *NiAs*, *GeP*, *BeO*, and *5-5* type polymorphs of ZnO at room temperature (300K) have been shown in Fig. 1(b). The dependence of the thermal conductivities on the chemical potential is the same as the σ/τ due to the equally dependence on the charge carriers. Similar to the σ/τ, the *CsCl*- and 5-5- types of ZnO type polymorph of ZnO exhibits larger κ/τ for *p*-type doping. Similarly, the NiAs type of ZnO exhibited larger κ/τ for *p*-type doping than *n*-type. Whereas larger values of κ/τ for the *wurtzite*, *CsCl*, *GeP*, *BeO*, and *5-5* type polymorphs of ZnO were recorded for their *n*-type doping than *p*-type. The maximum values of κ/τ and corresponding doping level determined for the *sphalerite*, *wurtzite*, *CsCl*, *NiAs*, *GeP*, *BeO*, and *5-5* type polymorphs of ZnO are tabulated in Table 1.

Table 1. The maximum values of σ/τ and κ/τ and corresponding chemical potentials, as well as the σ/τ and κ/τ calculated over Fermi level for sphalerite, wurtzite, CsCl, NiAs, GeP, BeO and 5-5 type polymorphs of ZnO

Prototype of ZnO	Electrical conductivity (σ/τ)			Thermal conductivity (κ/τ)		
	σ_{max}/τ ($\times 10^{20}$/Ωms)	μ (eV)	σ/τ ($\times 10^{20}$/Ωms) at Fermi level	κ_{max}/τ ($\times 10^{15}$ W/mKs)	μ (eV)	κ/τ ($\times 10^{15}$ W/mKs) at Fermi level
Wurtzite	7.13	6.64	5.49	5.22	6.71	3.92
Sphalerite	9.49	7.16	6.50	6.49	7.48	4.72
GeP	9.82	7.39	0.14	7.17	7.35	0.22
5-5	5.88	-2.79	0.11	4.25	-2.37	0.20
NiAs	7.60	6.54	0.02	9.96	-2.58	0.09
BeO	4.93	6.97	0.02	3.67	6.18	0.03
CsCl	8.10	-1.99	0.60	7.25	-2.81	0.70

Fig. 2 represents the Seebeck coefficients vs. chemical potential ($\mu(eV)$) for *sphalerite*, *wurtzite*, *CsCl*, *NiAs*, *GeP*, *BeO*, and *5-5* type polymorphs of ZnO at room temperature (300 K). The Seebeck effect occurs due to the temperature gradient between two points of a conductor which generates the electric voltage. The efficiency of the generated electric voltage due to the temperature gradient is known as the Seebeck coefficient [55].

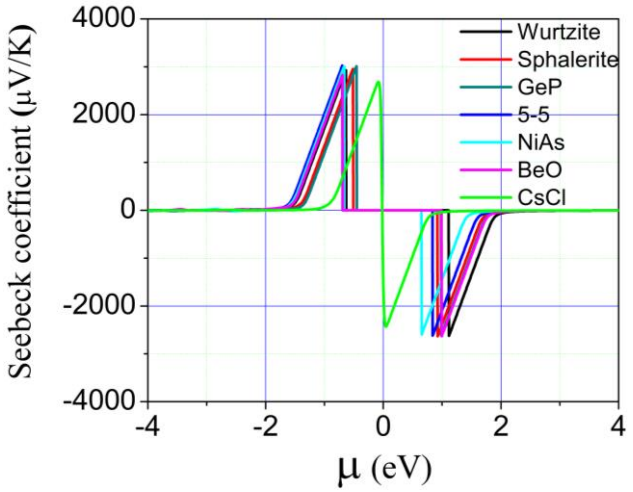

Fig. 2. Seebeck coefficients of wurtzite type, sphalerite type, GeP type, 5-5 type, NiAs type, BeO type, and CsCl type ZnO polymorphs against chemical potential (μ) (color online)

It is clear from Fig. 2 that the considered polymorphs mostly exhibit a relatively larger Seebeck coefficient in *n*-type doping. The maximum peak values of *sphalerite*, *wurtzite*, *CsCl*, *NiAs*, *GeP*, *BeO* and *5-5* type polymorphs of ZnO has been recorded as 2950 μK/V, 2950 μK/V, 2220 μK/V, 3000 μK/V, 3020 μK/V, 2830 μK/V and 3020 μK/V respectively. These calculated Seebeck coefficients are relatively larger than 2390.20 μV/K reported for wurtzite ZnO at 250 K [56]. The observed difference between the calculated Seebeck coefficients with that of the available literature can be attributed to the difference in the adopted methodologies.

It has been recorded that *CsCl* type polymorph exhibits a relatively smaller Seebeck coefficient value than the other polymorphs of ZnO. This can be attributed to the relatively larger σ/τ which confirms the inverse relation between electrical conductivity and Seebeck coefficient.

The power factors (*P.F*) against the chemical potential for *sphalerite*, *wurtzite*, *CsCl*, *NiAs*, *GeP*, *BeO* and *5-5* type polymorphs of ZnO at room temperature (300 K) are calculated by using the following relation and shown in Fig. 3:

$$P.F = S^2 \frac{\sigma}{\tau} \tag{5}$$

It is clear from Equation (5) that the power factor depends on the Seebeck coefficient (S) and electrical conductivity (σ/τ). Thus larger Seebeck coefficient and larger electrical conductivity can enhance the power factor individually or collectively. It can be seen from Fig. 3 all polymorphs of ZnO demonstrate power factors peaks mainly for *p*-type doping. Hence the power factors of all these polymorphs can be enhanced by *p*-type doping.

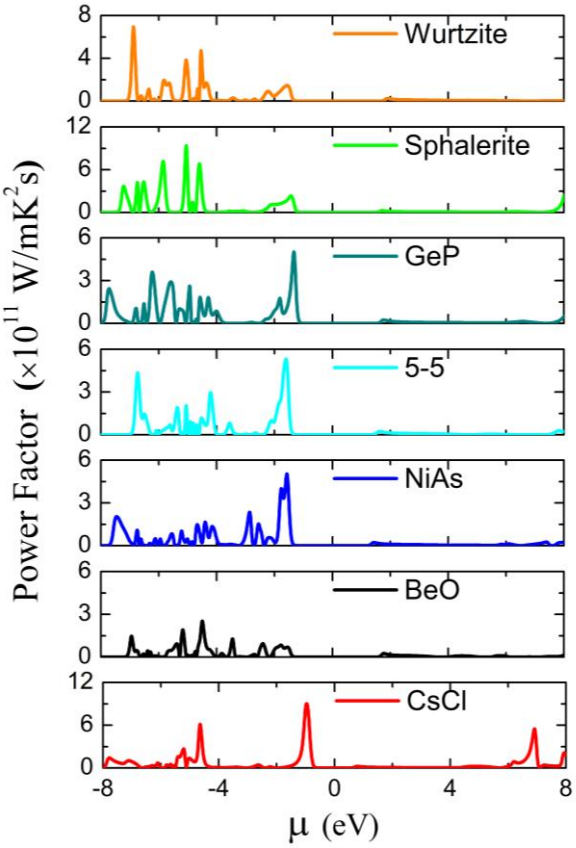

Fig. 3. Power factors of wurtzite type, sphalerite type, GeP type, 5-5 type, NiAs type, BeO type, and CsCl types of ZnO against chemical potential (μ) (color online)

The small peaks seen in the power factor for *n*-type doping for *wurtzite* and *sphalerite* types polymorphs of ZnO are the contribution of the σ/τ with the magnitudes of 1.77×10^{11} μ W/cm K^{2}s at 1.45 eV and 2.36×10^{11} μ W/cm K^{2}s at 1.41 eV respectively. In *CsCl*, *NiAs*, *GeP*, and *5-5* type polymorphs of ZnO, the maximum values of power factors ($P.F_{max}$) occur at relatively low doping level whereas *sphalerite*, *wurtzite*, and *BeO* type of ZnO showed their maximum power factor values relatively at high doping level. The $P.F_{max}$ of *sphalerite*, *wurtzite*, *CsCl*, *NiAs*, *GeP*, *BeO* and *5-5* type of the polymorphs of ZnO and the corresponding values of chemical potential ($\mu(eV)$), electrical conductivities (σ/τ), and Seebeck coefficients (S) are listed in Table 2.

Table 2. The maximum values of power factors ($P.F_{max}$) and the corresponding values of chemical potential (μ), electrical conductivity (σ/τ), and Seebeck coefficient (S) for sphalerite, wurtzite, CsCl, NiAs, GeP, BeO and 5-5 type polymorphs of ZnO

Prototype of ZnO	$P.F_{max}$ ($\times 10^{11}$ μ W/ cm K^{2}s)	μ (eV)	S (μK/V)	σ/τ ($\times 10^{20}$/Ωms)
Wurtzite	7.01	-3.63	-1700	0.239
Sphalerite	8.04	-2.11	-1800	0.234
GeP	4.97	-0.002	1600	0.172
5-5	5.31	-0.03	1300	0.278
NiAs	4.90	-0.08	1300	0.286
BeO	2.28	-3.04	-50	0.802
CsCl	11.7	-0.003	-90	0.688

Table 2 shows the largest power factor value for the *CsCl* polymorph of ZnO due to the corresponding high value of σ/τ while the *BeO* type polymorph of ZnO exhibits relatively smaller power factor owing to the fact of the smaller value of the Seebeck coefficient correspondingly.

In the rest of the part of this article, we discuss the effect of temperature on σ/τ, thermal conductivities, Seebeck coefficient, and power factor of *sphalerite*, *wurtzite*, *CsCl*, *NiAs*, *GeP*, *BeO*, *5-5* type of the polymorphs of ZnO over Fermi level. Fig. 4(a) represents the σ/τ vs. temperature for *sphalerite*, *wurtzite*, *CsCl*, *NiAs*, *GeP*, *BeO*, *5-5* polymorphs of ZnO. The *wurtzite* type *CsCl* polymorphs exhibit more sensitivity to the temperature gradient. It is recorded that the *wurtzite* type polymorph of ZnO displays highest σ/τ of magnitude 5.53 × 10^{20}/Ωms at less than room temperature which is decreasing with an increase in temperature. The *sphalerite* type, *NiAs* type, and *BeO* type polymorphs demonstrate insignificant increment in σ/τ with the increase in the temperature and the maximum values of σ/τ have been found as 0.15 × 10^{20}/Ωms, 0.13 × 10^{20}/Ωms, and 0.07 × 10^{20}/Ωms at 1000 K. The*GeP* type and *5-5* type polymorphs exhibit a minor increment with an increase in temperature; however, the increment is slightly larger than *sphalerite* type, *NiAs* type and *BeO* type polymorphs of ZnO. The maximum values of σ/τ for *GeP* type and *5-5* type have been recorded as 0.40 × 10^{20}/Ωms and 0.47 × 10^{20}/Ωms respectively at 1000K.

The σ/τ of *CsCl* type polymorph shows relatively better increment as compared to *sphalerite*, *NiAs*, *GeP*, *BeO* and *5-5* types ZnO polymorphs with the increase in temperature and the maximum value is recorded as 1.17 × 10^{20}/Ωms at the highest temperature. Fig. 4(b) depicts the κ/τ against temperature for *sphalerite*, *wurtzite*, *CsCl*, *NiAs*, *GeP*, *BeO*, *5-5* types polymorphs of ZnO for fixed chemical potential (Fermi level). From Figure.7, it is clear that *wurtzite* type polymorph has a rapid increase in κ/τ with the increase in temperature. *NiAs* and *BeO* type's polymorphs of ZnO have a very small effect on their thermal conductivities with the increase in temperatures. Similarly, *sphalerite*, *GeP*, and *5-5* types ZnO polymorphs also have a minor increment in κ/τ after 500 K. The κ/τ of the *CsCl* type polymorph is found to increase gradually with an increase in temperature.

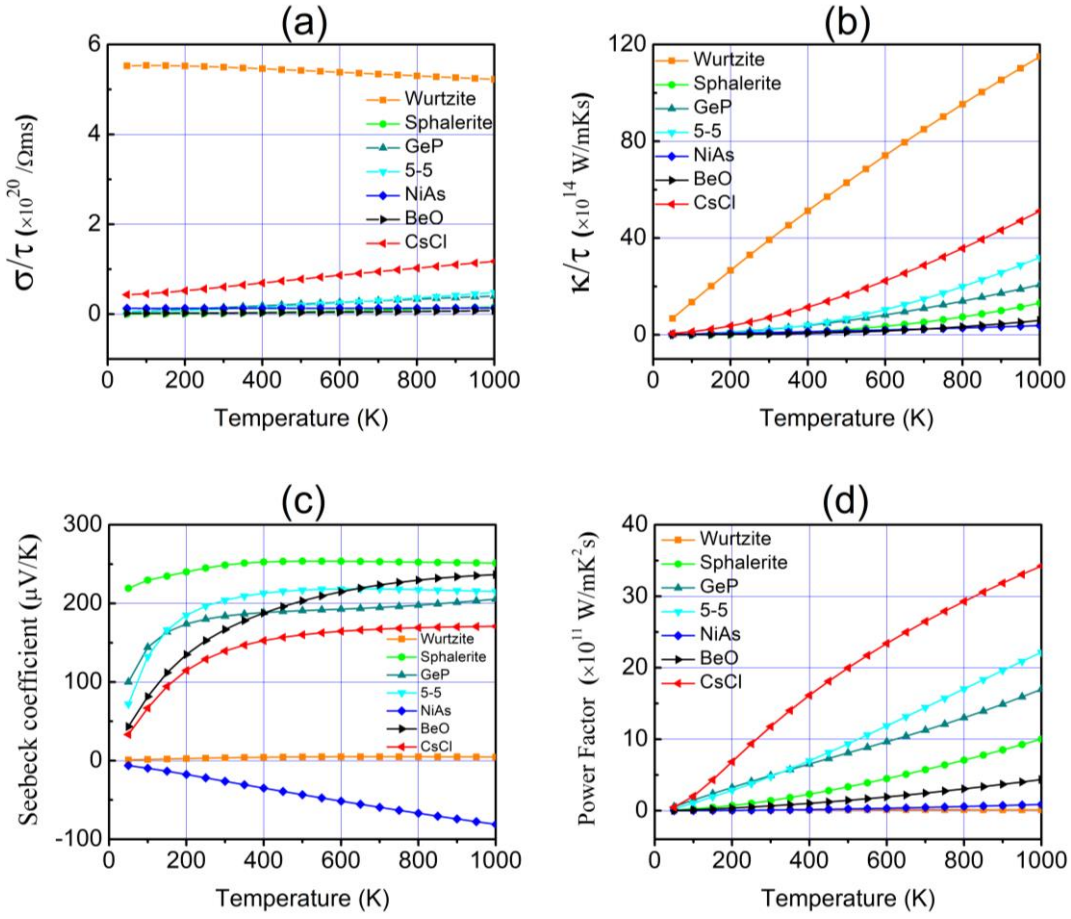

Fig. 4. σ/τ(a), κ/τ (b), Seebeck coefficient (c), and P.F (d) results for sphalerite, wurtzite, CsCl, NiAs, GeP, BeO, 5-5 type of the polymorphs of ZnO against temperature (K) (color online)

Fig. 4(c) shows the Seebeck coefficients (*S*) vs. temperature for *sphalerite*, *wurtzite*, *CsCl*, *NiAs*, *GeP*, *BeO*, *5-5* type of the polymorphs of ZnO. The *wurtzite* type polymorph of ZnO is showing a very small increment in the results of Seebeck coefficient with increasing temperature. The Seebeck coefficient of *sphalerite* type polymorph is found increasing below room temperature (300 K) but above room temperature, Seebeck coefficient values seem to be constant. On the other hand, *CsCl*, *GeP*, *BeO*, and *5-5* type's polymorphs have been found to experiencing a significant increase in the Seebeck coefficient below room temperature. Beyond room temperature, the increment in Seebeck coefficient is found gradually rising with increasing temperature for *BeO* type polymorph whereas for *CsCl* and *GeP* types show small increment in Seebeck coefficient beyond 300 K. The Seebeck coefficient of *5-5* type polymorph is increasing with the increase in temperature and it reaches a maximum value at 600 K and after 600 K, Seebeck coefficient is decreasing with increase in temperature. For the case of *NiAs* type, the Seebeck coefficient has been recorded to be decreased rapidly with an increase in temperature.

The effect of the temperature on the power factors of *sphalerite*, *wurtzite*, *CsCl*, *NiAs*, *GeP*, *BeO*, *5-5* type of the polymorphs of ZnO has been presented in Fig. 4(d). It can be seen clearly from Fig. 4(d) that *wurtzite* type polymorph has no effect of temperature on its power factor. It is recorded that above 450 K, *wurtzite* type polymorph has an extremely small increase in the order of 0.01×10^{12} μW/cmK^{2}s. This indicates that an increase in temperature does not affect the efficiency of *wurtzite* structured ZnO. Similarly, *NiAs* type polymorph has a small increment of power factor with an increase in temperature. *Sphalerite* type and *BeO* type polymorphs show a small increment in the results of the power factor above 300K and below it. Overall, it is increasing with the increase in temperature. *GeP* type and *5-5* type polymorphs of ZnO have a significant increment with increasing temperature even below the room temperature. However, a rapid increase in the power factor of *CsCl* has been observed with an increase in temperature.

4. Conclusion

In summary, we have presented the DFT based study of the thermoelectric properties for the *sphalerite*, *wurtzite*, *CsCl*, *NiAs*, *GeP*, *BeO*, *5-5* types polymorphs of ZnO by employing the semi-classical Boltzmann transport theory and DFT approaches. The thermoelectric coefficients of the thermal conductivity (κ/τ), electrical conductivity (σ/τ), power factor (P.F), and Seebeck coefficient (S) parameter for the *sphalerite*, *wurtzite*, *CsCl*, *NiAs*, *GeP*, *BeO* and *5-5* types ZnO polymorphs were calculated as a function of chemical potential (at room temperature) and temperature (0 to 1000 K). Our calculations of σ/τ to relaxation time (σ/τ) revealed that *wurtzite*, *CsCl*, *NiAs*, *GeP*, *BeO* and *5-5* types polymorphs exhibited larger σ/τ for *p*-type doping whereas the *sphalerite* type polymorph of ZnO showed larger σ/τ for *n*-type doping. With the increase in temperature, σ/τ of *wurtzite* ZnO was decreasing whereas the other polymorphs of ZnO exhibited increment in σ/τ with an increase in temperature. Similar to the σ/τ, the *sphalerite* polymorph has been recorded to exhibit larger thermal conductivity (κ/τ) for *n*-type doping whereas κ/τ results for *wurtzite*, *CsCl*, *NiAs*, *GeP*, *BeO* and *5-5* types polymorphs showed higher values for *p*-type doping. The calculations of Seebeck coefficients at room temperature showed that the considered polymorphs mostly exhibited the Seebeck coefficient in *n*-type doping. Only *wurtzite* type and *sphalerite* type structures of ZnO showed small peaks of the Seebeck coefficient in *p*-type doping. This study reveals that these new polymorphs of ZnO exhibit large power factor values and have great potential to be used as the thermoelectric materials.

Acknowledgment

The author (Bakhtiar Ul Haq) extends his appreciation to the Deanship of Scientific Research at King Khalid University, Saudi Arabia, for funding this work through the Research Groups Program under Grant No. R.G.P. 1/121/42.

References

[1] Y. Du, J. Xu, B. Paul, P. Eklund, Applied Materials Today **12**, 366 (2018).
[2] L. E. Bell, Science **321**(5895), 1457 (2008).
[3] B. Ul Haq, S. AlFaify, A. Laref, The Journal of Physical Chemistry C **123**(30), 18124 (2019).
[4] B. U. Haq, S. AlFaify, A. Laref, R. Ahmed, M. Taib, Ceramics International **45**(12), 15122 (2019).
[5] B. U. Haq, S. AlFaify, A. Laref, Physical Chemistry Chemical Physics **21**(8), 4624 (2019).
[6] C. Fu, S. Bai, Y. Liu, Y. Tang, L. Chen, X. Zhao, T. Zhu, Nature Communications **6**, 8144 (2015).
[7] F. K. Butt, B. U. Haq, S. Ur Rehman, R. Ahmed, C. Cao, S. AlFaifi, Journal of Alloys and Compounds **715**, 438 (2017).
[8] T.-B. Hur, G. S. Jeen, Y.-H. Hwang, H.-K. Kim, Journal of Applied Physics **94**(9), 5787 (2003).
[9] Ü. Özgür, Y. I. Alivov, C. Liu, A. Teke, M. Reshchikov, S. Doğan, V. Avrutin, S.-J. Cho, H. Morkoç, Journal of Applied Physics **98**(4), 11 (2005).
[10] Z. Zhou, K. Kato, T. Komaki, M. Yoshino, H. Yukawa, M. Morinaga, K. Morita, Journal of the European Ceramic Society **24**(1), 139 (2004).
[11] N. L. Hadipour, A. Ahmadi Peyghan, H. Soleymanabadi, The Journal of Physical Chemistry C **119**(11), 6398 (2015).
[12] C. R. A. Catlow, S. A. French, A. A. Sokol, A. A. Al-Sunaidi, S. M. Woodley, Journal of Computational Chemistry **29**(13), 2234 (2008).
[13] Z. Zeng, C. S. Garoufalis, S. Baskoutas, G. Bester,

Physical Review B **87**(12), 125302 (2013).
[14] A. Kronenberger, A. Polity, D. M. Hofmann, B. K. Meyer, A. Schleife, F. Bechstedt, Physical Review B **86**(11), 115334 (2012).
[15] F. Raffone, F. Risplendi, G. Cicero, Nano Letters **16**(4), 2543 (2016).
[16] T. Pauporté, O. Lupan, J. Zhang, T. Tugsuz, I. Ciofini, F. D. R. Labat, B. Viana, ACS Applied Materials & Interfaces **7**(22), 11871 (2015).
[17] J. Lee, D. C. Sorescu, X. Deng, The journal of Physical Chemistry Letters **7**(7), 1335 (2016).
[18] M. Sardarabadi, M. Passandideh-Fard, M.-J. Maghrebi, M. Ghazikhani, Solar Energy Materials and Solar Cells **161**, 62 (2017).
[19] J. Xu, Z. Xue, N. Qin, Z. Cheng, Q. Xiang, Sensors and Actuators B: Chemical **242,** 148 (2017).
[20] L. Liu, Z. Mei, A. Tang, A. Azarov, A. Kuznetsov, Q.-K. Xue, X. Du, Physical Review B **93**(23), 235305 (2016).
[21] X. Wang, K. Chen, Y. Zhang, J. Wan, O. L. Warren, J. Oh, J. Li, E. Ma, Z. Shan, Nano Letters **15**(12), 7886 (2015).
[22] M. Ohtaki, T. Tsubota, K. Eguchi, H. Arai, Journal of Applied Physics **79**(3), 1816 (1996).
[23] J. Wiff, Y. Kinemuchi, H. Kaga, C. Ito, K. Watari, Journal of the European Ceramic Society **29**(8), 1413 (2009).
[24] B. Ul Haq, A. Afaq, R. Ahmed, S. Naseem, International Journal of Modern Physics C **23**(06), 1250043 (2012).
[25] U. H. Bakhtiar, R. Ahmed, R. Khenata, M. Ahmed, R. Hussain, Materials Science in Semiconductor Processing **16**(4), 1162 (2013).
[26] B. Ul Haq, R. Ahmed, S. Goumri-Said, A. Shaari, A. Afaq, Phase Transitions **86**(12), 1167 (2013).
[27] B. U. Haq, R. Ahmed, S. Goumri-Said, Solar Energy Materials and Solar Cells **130**, 6 (2014).
[28] D. Zagorac, J. C. Schön, I. V. Pentin, M. Jansen, Process. Appl. Ceram. **5**, 73 (2011).
[29] D. Zagorac, J. Schön, J. Zagorac, M. Jansen, Physical Review B **89**(7), 075201 (2014).
[30] D. Zagorac, J. Schön, K. Doll, M. Jansen, Acta Physica Polonica A **120**(2), 215 (2011).
[31] S. Shabbir, A. Shaari, B. U. Haq, R. Ahmed, M. Ahmed, Optik **206**, 164285 (2020).
[32] P. Blaha, K. Schwarz, G. K. Madsen, D. Kvasnicka, J. Luitz, Wien2k. An augmented plane wave+ local orbitals program for calculating crystal properties, Vienna University of Technology, Austria, (2001).
[33] G. K. Madsen, D. J. Singh, Computer Physics Communications **175**(1), 67 (2006).
[34] D. Koller, F. Tran, P. Blaha, Physical Review B **85**(15), 155109 (2012).
[35] B. U. Haq, R. Ahmed, J. Y. Rhee, A. Shaari, S. AlFaify, M. Ahmed, Journal of Alloys and Compounds **693**, 1020 (2017).
[36] S. Shabbir, A. Shaari, B. U. Haq, R. Ahmed, S. AlFaify, M. Ahmed, A. Laref, Materials Science in Semiconductor Processing **121**, 105326 (2021).
[37] B. U. Haq, R. Ahmed, A. Shaari, A. Afaq, B. Tahir, R. Khenata, Materials Science in Semiconductor Processing **29**, 256 (2015).
[38] B. U. Haq, S. AlFaify, T. Alshahrani, R. Ahmed, F. K. Butt, S. U. Rehman, Z. Tariq, Solar Energy **211**, 920 (2020).
[39] B. U. Haq, S. AlFaify, T. Alshahrani, R. Ahmed, S. Tahir, N. Amjed, A. Laref, Results in Physics **19**, 103367 (2020).
[40] B. U. Haq, S. AlFaify, T. Al-shahrani, S. Al-Qaisi, R. Ahmed, A. Laref, S. Tahir, Journal of Physics and Chemistry of Solids **149**, 109780 (2021).
[41] B. U. Haq, R. Ahmed, S. Goumri-Said, Materials Research Express **1**(1), 016108 (2014).
[42] B. U. Haq, R. Ahmed, G. Abdellatif, A. Shaari, F. K. Butt, M. B. Kanoun, S. Goumri-Said, Frontiers of Physics **11**(1), 117101 (2016).
[43] B. U. Haq, A. Afaq, R. Ahmed, S. Naseem, Chinese Physics B **21**(9), 097101 (2012).
[44] B. U. Haq, R. Ahmed, A. Shaari, N. Ali, Y. Al-Douri, A. Reshak, Materials Science in Semiconductor Processing **43**, 123 (2016).
[45] B. U. Haq, S. AlFaify, T. Al-shahrani, S. Al-Qaisi, R. Ahmed, A. Laref, S. Tahir, Journal of Physics and Chemistry of Solids **149**, 109780 (2020).
[46] B. U. Haq, S. AlFaify, T. Alshahrani, R. Ahmed, Q. Mahmood, D. Hoat, S. Tahir, Physica E: Low-dimensional Systems and Nanostructures **126**, 114444 (2021).
[47] B. U. Haq, S. AlFaify, R. Ahmed, A. Laref, Q. Mahmood, E. Algrafy, Applied Surface Science **525**, 146521 (2020).
[48] B. U. Haq, S. AlFaify, A. S. Jbara, R. Ahmed, F. K. Butt, A. Laref, A. R. Chaudhry, Z. A. Shah, Ceramics International **46**(14), 22181 (2020).
[49] S. Shabbir, A. Shaari, B. U. Haq, R. Ahmed, S. AlFaify, M. Ahmed, A. Laref, Materials Science in Semiconductor Processing **121**, 105326 (2021).
[50] S. Shabbir, A. Shaari, B. U. Haq, R. Ahmed, S. AlFaify, M. Ahmed, A. Laref, Materials Science in Semiconductor Processing **121**, 105326 (2020).
[51] S. Shabbir, A. Shaari, B. U. Haq, R. Ahmed, S. AlFaify, M. Ahmed, A. Laref, Materials Science and Engineering: B **262**, 114697 (2020).
[52] B. Ul Haq, S. AlFaify, R. Ahmed, F. K. Butt, A. Laref, S. Goumri-Said, S. Tahir, Journal of Applied Physics **123**(17), 175107 (2018).
[53] U. Ozgur, D. Hofstetter, H. Morkoc, Proceedings of the IEEE **98**(7), 1255 (2010).
[54] Ü. Özgür, Y. I. Alivov, C. Liu, A. Teke, M. Reshchikov, S. Doğan, V. Avrutin, S.-J. Cho, Morkoç, Journal of Applied Physics **98**(4), 11 (2005).
[55] K. Uchida, S. Takahashi, K. Harii, J. Ieda, W. Koshibae, K. Ando, S. Maekawa, E. Saitoh, Nature **455**(7214), 778 (2008).
[56] P. Sikam, C. Sararat, P. Moontragoon, T. Kaewmaraya, S. Maensiri, Applied Surface Science **446**, 47 (2018).

*Corresponding author: bakhtiarjadoon@gmail.com